Journal of Applied Polymer Science

Preparation of Polyamidoamine Dendrons Supported on Chitosan Microspheres and the Adsorption of Bilirubin

Liping Wu,[1] Zhengpu Zhang[2]

[1]Department of Experimental Teaching, Tianjin University of Traditional Chinese Medicine, Tianjin 300193, People's Republic of China

[2]Institute of Polymer Chemistry, Key Laboratory of Functional Polymeric Materials, Nankai University, Tianjin 300071, People's Republic of China

Correspondence to: L. Wu (E-mail: 272847684@qq.com)

ABSTRACT: The aim of this study was to prepare a new adsorbent for bilirubin (BR); low generation (G, G $\leq$4) hexanediamine-containing polyamidoamine (PAMAM) dendrons were supported on chitosan (CS) microspheres (CS-Gn, n = 0,1,2,3,4). The adsorption properties of this novel adsorbent for BR in aqueous solution were examined. The adsorption percentages were over 70% at 0.5 h and over 90% at 1 h. The adsorption capacity was up to 43 mg/g and was not yet saturated. The BR adsorption increased with increasing temperature and increasing BR initial concentration and was the highest at pH 7.4; it decreased slightly with increasing ionic strength and occurred even in the presence of bovine serum albumin (BSA). We observed that the CS–Gn microspheres had satisfactory competitive abilities with BSA, although the adsorption percentage decreased a certain extent in the presence of BSA. In addition, the CS–Gn microspheres were easier to prepare than the usual PAMAM dendrimers. In summary, this adsorbent is a promising biomedical material for BR removal for artificial liver supported systems. © 2013 Wiley Periodicals, Inc. J. Appl. Polym. Sci. 000: 000–000, 2013

KEYWORDS: adsorption; dendrimers; hyperbranched polymers and macrocycles; polyamides; resins

Received 20 November 2012; accepted 16 February 2013; published online
DOI: 10.1002/app.39193

INTRODUCTION

Bilirubin (BR) is the normal metabolic product of hemoglobin in decrepit red blood cells and has a molecular weight (MW) of 584. The chemical structure of BR is shown in Scheme 1. It exists mainly in two forms in the human body: the free form (called *direct BR*) and the form combined with serum albumin or glucuronic acid (called *indirect BR*). Free BR is a lipophilic endotoxin, so it is insoluble under physiological conditions in the body. Under normal circumstances, free BR is combined with human serum albumin in the blood to form water-soluble complexes and transported to the liver through the blood; once in the liver, it separates from albumin, conjugates with glucuronic acid to form more water-soluble complexes, and is then excreted into the bile by the liver cells. Finally, it is excreted out of the body through further metabolism so a normal concentration of BR in the body can be maintained. However, when one or a few steps of BR metabolism are obstructed, this will result in a total serum BR concentration (of the direct and indirect forms) exceeding the normal level and will further cause hyperbilirubinemia (jaundice), especially in newborn infants. Free BR can pass through the cell membrane and the blood–brain barrier, so this can lead further to cell death in all kinds of organs, especially brain cells, and can lead to mental retardation, cerebral palsy, or even death. It can also cause liver or bile duct dysfunction and aggravate hepatic injury, particularly in hepatitis patients. Therefore, the serum BR concentration is an important index for identifying various liver diseases.

Scientists have used a variety of methods to remove excess BR in the body. In recent years, many technologies for hyperbilirubinemia treatment have been developed; these include light therapy and blood purification therapies, including plasma exchange (plasmapheresis),[1] plasmadialysis, plasma perfusion, plasma hemoperfusion, hemodialysis, hemofiltration, hemodiafiltration, molecular adsorbent recirculating system,[2–10] and the Prometheus system.[4,9,10] The investigation of BR adsorbents is a hot research topic for BR removal. Reported adsorbents[11–33] have included mainly polymer microbeads,[11,15–18,30] membranes,[12,19,20] fibers,[28,29] and amorphous materials.[13,14,21–27,31–33] The adsorbents used in blood purification should be safe and nontoxic to bodies, possess stable chemical properties, good biocompatibility (especial blood compatibility), large adsorption capacity, and high mechanical strength.[34] So far, the main

Applied Polymer SCIENCE

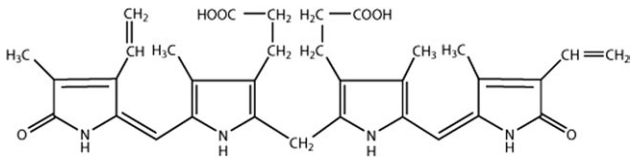

Scheme 1. Chemical structure of BR.

problems of the adsorbents used in clinical environments are poor blood compatibility and low adsorption capacity. So, in this study, chitosan (CS), a natural, nontoxic polymer with good biocompatibility, was used as a base material.

In our previous work,[34] hexanediamine (HDA)-modified CS and a series of low generation ($\leq$ 3) ethylenediamine (EDA)-containing PAMAM dendrons supported on CS were prepared for BR adsorption. The results showed that CS–HDA had the best adsorption properties, even when the content of the amino groups was not very high. So, in this study, a series of low generation (G, G$\leq$4) HDA-containing PAMAM dendrons supported on CS were synthesized. It was difficult to directly support PAMAM–G2.0 or PAMAM–3.0 dendrons on CS,[34] so in this study, HDA-modified CS was used as the reactive core, and CS-supported, HDA-containing PAMAM dendrons were obtained by the divergent method used in the preparation of PAMAM dendrons.[35] The advantages of this method were as follows: (1) the separation and purification of the products were simplified as they could be achieved by simple filtration (2) the conversion percentage could be improved with a great excess of reagents, and (3) the unreacted reagents could easily be recycled. The results show that all of the adsorption capacities of CS–HDA–G1.0–G4.0 were higher than that of CS–HDA. In our previous study, the saturated adsorption capacity of EDA-containing PAMAM dendrons was 15 mg/g. In this study, the adsorption capacity of the HDA-containing PAMAM dendrons was 43 mg/g, and they were not yet saturated.

EXPERIMENTAL

Materials

A BR (>95%) solution (100 mg/L) was prepared by the dissolution of BR into a sodium hydroxide aqueous solution (0.1 mol/L) and dilution with a phosphate buffer solution (0.05 mol/L, pH = 7.2–7.4) before use in a dark room. All BR solutions were stored in amber glass vials wrapped with aluminum foil and placed in the dark to prevent light-initiated BR oxidation. A CS (10.6×10^4 Da, 85% degree of deacetylation) aqueous solution (5% w/w) was prepared by the dissolution of CS into an acetic acid aqueous solution (2% v/v). Methyl acrylate (MA) was distilled *in vacuo* before use. Bovine serum albumin (BSA) fraction V (MW = 68000 Da) was purchased from Roche, Basel, Switzerland. Gn's of HDA-containing PAMAM dendrons supported on CS microspheres were prepared with 1,6-HDA and MA according to a method reported previously.[35] All other chemicals were analytical grade and were purchased from the Sixth Chemical Reagent Factory (Tianjin, China).

Scanning electron microscopy (SEM; S-3500N, Hitachi, Tokyo, Japan) and Fourier transform infrared (FTIR) spectroscopy (FTS 6000, Bio-Rad, Hercules, California, USA) were used to characterize the structure of the functionalized crosslinked CS microspheres. The amino content of the microspheres was determined by a method reported previously.[36] The nitrogen and chlorine contents of the microspheres were determined with an elemental analyzer (Elementar Vario EL, Germany) and the Volhard method, respectively. BR adsorption experiments were carried out in a constant-temperature immersion oscillator (SHZ-88, Jintan Medical Instrument Factory, Jintan, China). The concentration of BR was determined by a UV-2450 spectrophotometer (Shimadzu, Kyoto, Japan) at 438 nm.

Preparation of the Microspheres

Mixtures of carbon tetrachloride and liquid paraffin (200 mL, 1:1 v/v) containing span-80 (0.47 g) were added to a 500-mL, three-necked, round-bottom flask with a mechanical stirrer. A CS (10.6×10^4 Da, 85% degree of deacetylation) aqueous solution [100 mL, 5% w/w, prepared by the dissolution of CS into an acetic acid aqueous solution (2% v/v)] was added to the flask with a stirring speed of 80 rpm and was reacted for 1 h at room temperature. The CS aqueous solution was dispersed into uniform beads with appropriate size. A formaldehyde aqueous solution (2 mL, 37% w/w) was added dropwise and reacted for 1 h. When the reaction temperature was raised to 40°C, a glutaraldehyde aqueous solution (7 mL, 50% w/w) was added dropwise and reacted for 2 h. Changing the amount of glutaraldehyde allowed us to obtain different crosslinked CS microspheres. When the reaction temperature was raised to 60°C, a sodium hydroxide aqueous solution (10% w/w) was added dropwise to adjust the pH value to 9–10; this was then reacted for 12 h for solidification. The products were filtered and washed with petroleum ether, ethanol (EtOH), and deionized water to remove liquid paraffin, span-80, and sodium hydroxide, respectively. We removed formaldehyde protection from CS by soaking the CS in an HCl solution (0.5 mol/L) at room temperature for 24 h to release more amino groups. Finally, the microspheres were dried *in vacuo* at 40°C (Scheme 2).

CS with formaldehyde protection (16 g, ~5 mmol/g —CH_2OH), epichlorohydrin (80 mL, 94.4 g, 1.02 mol), and water (60 mL) were added to a 250-mL, three-necked, round-bottom flask, and the mixture was stirred mechanically at 60°C for 0.5 h. Perchloric acid (16 mL, 28.3 g, 0.2 mol) was added dropwise to the flask with caution. After 8 h, the product was filtered and

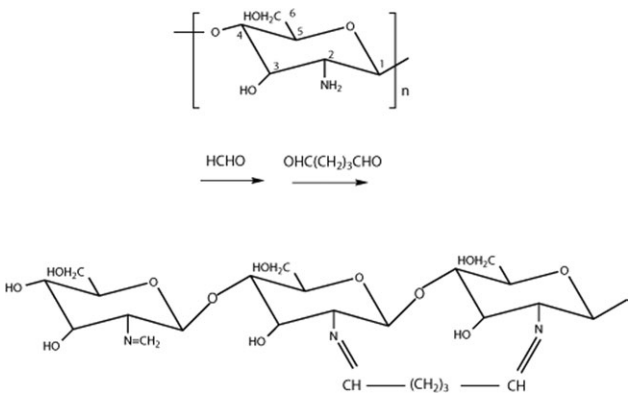

Scheme 2. Preparation of the glutaraldehyde crosslinked macroporous CS.

washed with acetone and water until it was neutral. Finally, the product was dried *in vacuo* at 40°C to obtain hydroxypropyl chlorinated chitosan (HPCS) microspheres. The chlorine content of HPCS was determined by the Volhard method.

HPCS (12 g, 1.74 mmol/g chlorine) and HDA (30 mL, 25.5 g, 0.22 mol) were added to a 100-mL, three-necked, round-bottom flask with mechanical stirring and reacted at 60°C for 24 h. The product was filtered and washed with acetone and then water until it was neutral. Finally, the microspheres were removed from the formaldehyde protection and dried *in vacuo* at 40°C to obtain CS–G0. The chlorine and nitrogen contents of CS–G0 were determined by the Volhard method and elemental analysis (Elementar Vario EL), respectively. The amino content was determined by a method reported previously.[36]

CS–G0 without formaldehyde protection (11 g, about 4.94 mmol/g of —NH_2), MA (25 mL, 23.75 g, 0.276 mol), and EtOH (40 mL) were added to a 250-mL, three-necked, round-bottom flask with mechanical stirring and argon protection at room temperature and were reacted for 24 h. The product was filtered and washed with EtOH. The final products were dried *in vacuo* at 40°C to obtain CS–G0.5. The nitrogen and amino contents were determined in the same way as those for CS–G0.

The mixture of HDA (150 mL, 127.5 g, 1.097 mol) and EtOH (100 mL) was cooled to room temperature, and then added to the mixture of CS–G0.5 (10 g, ~2.2 mmol/g of —$COOCH_3$) and EtOH (60 mL) in a 500-mL, three-necked, round-bottom flask under mechanical stirring and argon protection. The mixture was stirred strongly at 0°C for 1 h and then reacted at room temperature for 96 h. The product was filtered, washed until it was neutral, and immersed in EtOH several times. The final products were dried *in vacuo* at 40°C to obtain CS–G1.0. The determination of the nitrogen and amino contents were done in the same way as those for CS–G0. The CS–G1.5 to CS–G4.0 microspheres were prepared by the same method. The reaction times for the preparation of CS–G2.0, CS–G3.0, and CS–G4.0 were 5, 6, and 7 days, respectively (Scheme 3).

Absorption of BR in Aqueous Solution

The dried microspheres (0.1 g, 80–100 mesh) and BR solution (10 mL, 100 mg/L, freshly prepared) were added to an amber glass vial wrapped with aluminum foil to carry out the adsorption experiments at 37°C in a constant-temperature immersion oscillator. There was a certain amount of attenuation because of the instability of the BR solution, so it was essential to use the initial BR solution as a blank reference. The concentration of BR was detected with a UV-2450 spectrophotometer (Shimadzu, Kyoto, Japan) at 438 nm for free BR and 460 nm for conjugated BR with BSA (MW = 68000 Da, Roche).

RESULTS AND DISCUSSION

Preparation of the Microspheres

An SEM photo of the CS (Figure 1) showed that the CS beads had a good spherical shape and were almost uniform particle size with only small dispersion. There was no aggregation of CS beads. The mean particle size of CS beads was 130 μm, and the particle size was mainly distributed between 80 and 150 μm. Under the same magnification, the mean particle size of the CS–G4.0 beads was 160 μm, apparently bigger than the CS beads; the particle size was mainly distributed between 110 and 190 μm. There were a few broken microspheres, but these should have no influence on the use of CS.

The amino content of the CS beads after the removal of the formaldehyde protection was 3.25 mmol/g (Table I).

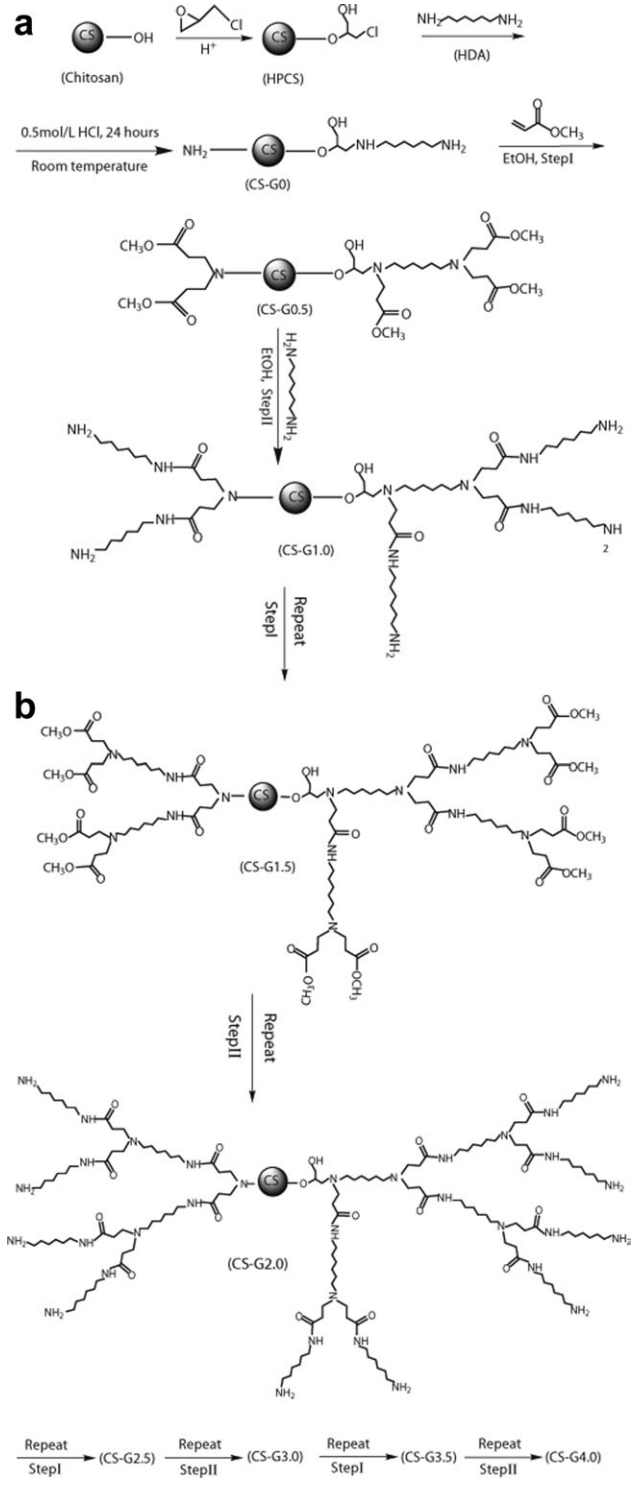

Scheme 3. Ideal synthetic route of CS–HDA–Gn.0.

Applied Polymer SCIENCE

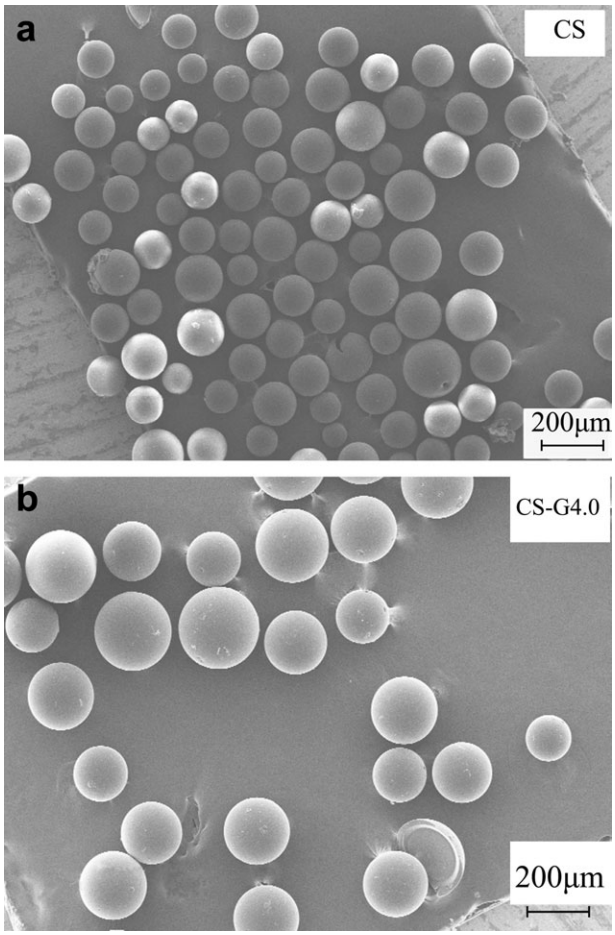

Figure 1. SEM photo of the CS and CS–G4.0 microspheres.

The FTIR spectrum of HPCS [with formaldehyde protection; Figure 2(a)] showed that the C—Cl absorption peak of HPCS appeared at 625 cm^{-1}. The chlorine content was 1.74 mmol/g.

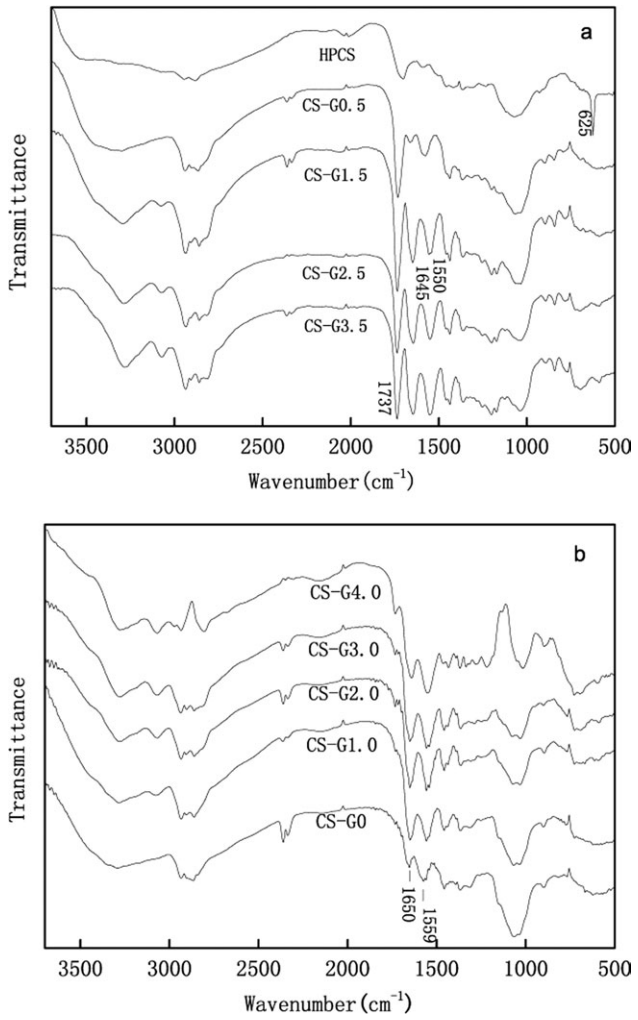

Figure 2. FTIR spectrum of the microspheres: (a) HPCS and CS–Gn.5 and (b) CS–Gn.0.

Table I. Characterization of the Microspheres[a]

Sample[a]	GP (%; Gn → Gn.5) Observed[b]	GP (%; Gn → Gn.5) Theoretical	N%	Amino content (mmol/g)
CS	—	—	5.06	3.25
HPCS	—	—	4.79	3.13
CS-G0	—	—	8.12	4.94
CS-G0.5	23.60	67.15	6.57	3.30
CS-G1.0	11.75	39.2	10.28	5.23
CS-G1.5	21.11	57.74	8.11	3.89
CS-G2.0	13.10	35.73	12.02	5.17
CS-G2.5	28.56	53.94	9.35	3.51
CS-G3.0	11.91	34.19	12.81	4.93
CS-G3.5	23.89	52.23	10.34	3.63
CS-G4.0	9.48	34.30	13.07	4.68

[a]80—100 mesh, with the removal of the formaldehyde protection.
[b]Calculated by the change in the nitrogen content on the microspheres from Gn to Gn.5.

The nitrogen content of CS (Table I) after the reaction with epichlorohydrin decreased slightly from 5.06 to 4.79%. All of the previous data proved the success of hydroxypropyl chlorination.

Compared with the FTIR spectrum of HPCS, the spectrum of CS–G0 [Figure 2(b)] showed that the C—Cl absorption peak of HPCS at 625 cm^{-1} disappeared; this echoed the chlorine content in CS–G0, which decreased from 1.74 to 0.06 mmol/g in HPCS. The details in the FTIR characterizations of CS–G0 to CS–G4.0 changed alternately and repeatedly with increasing generations. All of the FTIR spectra of CS–Gn.5 [Figure 2(a)] were similar: the strong characteristic absorption peak of C=O in ester groups of PAMAM dendrons appeared near 1737 cm^{-1} [Figure 2(a)], and the characteristic absorption peak of C=O in the imido groups of the PAMAM dendrons was present at 1645 cm^{-1} (except in CS–G0.5). All of the FTIR spectra of the CS–Gn.0 [Figure 2(b)] were similar: the characteristic absorption peak of C=O in the imido groups of the PAMAM dendrons presented at 1650 cm^{-1} [the weak one in the CS–G0 spectrum was that of the residual acetyl imido group because of the incomplete deacetylation; Figure 2(b)]; that of C=O in the

ester groups of the PAMAM dendrons disappeared at 1737 cm^{-1}; this proved that CS–Gn.5 was basically transformed to the corresponding CS–Gn.0 after the reaction. So, from the previous analysis, it was proven that PAMAM dendrons could be successfully loaded onto the surface of CS beads by an alternate and repeated reaction of Michael addition and ester aminolysis.

The amino and nitrogen contents on HPCS (Table I) after the reaction with HDA increased obviously. The amino and nitrogen content on CS–G0–G4.0 changed alternately and repeatedly with increasing generations. Moreover, the amino and nitrogen contents on all of the whole generations of CS–Gn.0 after the reaction with MA decreased obviously, whereas that on all of the half generations of CS–Gn.5 after the reaction with HDA increased obviously. The previous analysis further proved the success of the preparation of the PAMAM dendrons supported on the CS beads.

The amino content on the whole generations of CS–G0 to CS–G4.0 first increased then decreased with increasing generations. This result may have been caused by the fact that the six-carbon chain of the HDA monomer led to an increase in the branched degree with increasing generations; this resulted in the earlier appearance of reactive steric hindrance and a decreasing reaction rate. The amino contents of CS–G2.0, CS–G3.0, and CS–G4.0 were higher than those of the corresponding CS–G1.5, CS–G2.5, and CS–G3.5; this proved that the aminolysis reactions of CS–G1.5, CS–G2.5, and CS–G3.5 with HDA did occur, although the amino content decreased with increasing generations.

Grafting Percentage (GP). The GP of every reaction step was determined with the following equation:

$$GP(\%) = (A/B) \times 100$$

where A is the weight of MA or HDA grafted onto CS and B is the weight of CS charged. A was calculated by the change in the nitrogen content (Table I) on the microspheres before and after the reaction. For example, in the reaction of CS–G0 → CS–G0.5, when CS–G0 was defined as 1 g, 0.236 g of MA grafted onto CS–G0.5 would be obtained by the change in the nitrogen content from 8.12 to 6.57%. The GP of CS–G0 → CS–G0.5 was obviously 23.6%.

The initial theoretical GP (CS–G0 → CS–G0.5) was calculated by the amino content of CS–G0. The following theoretical GP was calculated by the stoichiometric proportion of every reaction step. The amino content of CS–G0 included the amount of —NH (from HDA) and $—NH_2$ (from CS and HDA). The amount of $—NH_2$ from CS was determined by the difference in the amino content of CS–G0 before and after the removal of formaldehyde protection. Then, the amount of —NH was calculated. The theoretical amount of MA grafted onto CS–G0 was calculated.

The GP of each reaction step is shown in Table I. The theoretical GP of CS-Gn.5 was similar and the same phenomenon of CS-Gn.0 appeared. The observed GP showed the same tendency, except for CS–G4.0. We concluded the success of every reaction step of the preparation of CS–G0–G4.0. It was shown that the observed GP was smaller than the theoretical GP, especially in CS–G4.0, and this could be explained by the effect of steric hindrance.

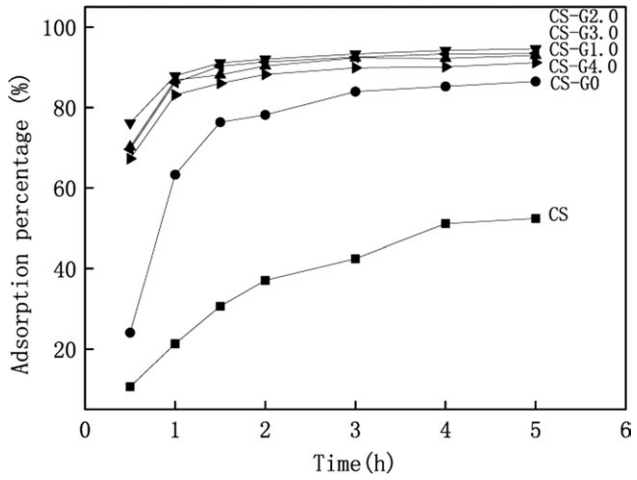

Figure 3. BR adsorption dynamic curves on microspheres: BR initial concentration = 100 mg/L; BR solution volume = 10 mL; microsphere weight = 0.1 g; pH 7.2–7.4; phosphate buffer concentration = 0.05 mol/L; temperature = 37°C; detected wavelength = 438 nm; size of the microspheres = 80–100 mesh.

Adsorption Experiment for BR

Adsorption Kinetics for BR. The order of the adsorption percentage of BR on the CS–Gn microspheres (Figure 3) was as follows: CS–G2.0, CS–G3.0, CS–G1.0, CS–G4.0 > CS–G0 > CS. The corresponding adsorption percentages were 95, 93, 93, 91, 86, and 52%, respectively. The adsorption percentages of CS–G1.0 to CS–G4.0 were similar. All of the microspheres except for CS arrived at equilibrium in about 2 h. The adsorption percentage of CS–G1.0to CS–G4.0 exceeded 70% at 0.5 h and were close to equilibrium at 1 h. We found that the adsorption capacity of all of the modified microspheres for BR, including the adsorption rate, adsorption percentage, and adsorption equilibrium time, was obviously higher than that of the unmodified CS. All of the adsorption capacities of CS–G1.0 to CS–G4.0 were higher than that of CS–G0. In our previous study,[34] the adsorption percentage of CS–HDA (CS–G0) was higher than CS–EDA–G0–G3.0. Therefore, this proved that the adsorption capacity for BR of CS–HDA–Gn.0 was much higher than that of CS–EDA–Gn.0, although the amino content of CS–HDA–Gn.0 was lower than that of CS–EDA–Gn.0;this was probably caused by the hydrophobic six-carbonic chain of HDA. The adsorption percentage first increased and then decreased with increasing generations. This result was probably due to the high steric hindrance of high generations; this led the BR molecules to be absorbed only on the surface of microspheres by the end amino groups, and this made it hard for them to enter the interior.

Effect of the Temperature. The adsorption percentages for BR at equilibrium on CS–G2.0 at 4, 25, and 37°C (Figure 4) were 87, 91, and 97%, respectively. The adsorption percentage increased with increasing temperature. However, the adsorption caused by hydrogen bonding and electrostatic interaction always

Applied Polymer SCIENCE

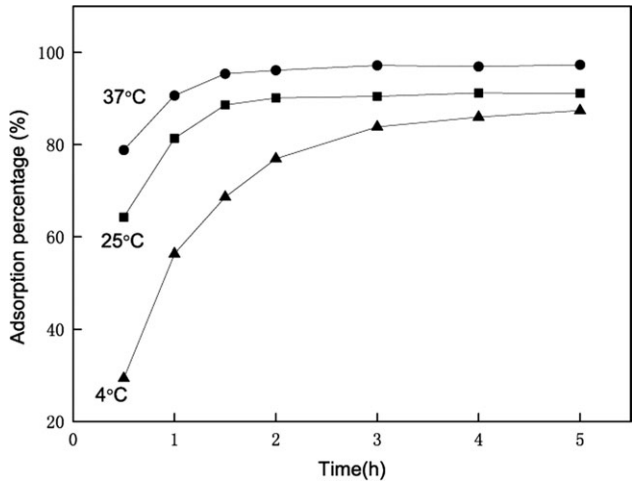

Figure 4. Effect of the temperature on the BR adsorption: BR initial concentration = 100 mg/L; BR solution volume = 10 mL; microsphere weight = 0.1 g; pH 7.2–7.4; phosphate buffer concentration = 0.05 mol/L; detected wavelength = 438 nm; microspheres = CS–G2.0, size of the microspheres = 80–100 mesh.

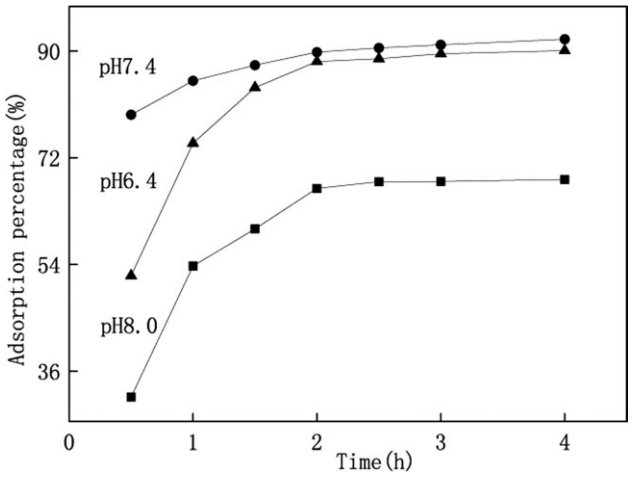

Figure 5. Effect of pH on the BR adsorption: BR initial concentration = 100 mg/L; BR solution volume = 10 mL; microsphere weight = 0.1 g; temperature = 37°C; detected wavelength = 438 nm; microspheres = CS–G2.0, size of the microspheres = 80–100 mesh.

decreased with increasing temperature because of the exothermic process. Therefore, the effect of temperature should have been caused by the hydrophobic interaction. The final effect of the temperature on adsorption was dependent on the result of the offset of the previous two effects. Hydrophobic interactions were more important for BR adsorption because BR was liposoluble. Thus, hydrophobic interaction was the key factor considered in the synthesis of CS–Gn.0 in this study. An increase in the temperature increased the contact area between the microspheres and BR, and it finally led to an increase in the adsorption rate. Another reason may have been that an increase in the temperature sped up the diffusion of BR molecules toward the adsorbent surface and increased the degree of swelling of the microspheres, so the contact area between the adsorbent and BR was increased, and the resistance of BR diffusing into microspheres was reduced. All of the previous phenomena led to an increase in the adsorption rate. The final reason may have been that an increase in temperature led to the change in the molecular configuration of BR from cis to trans, which reduced the steric hindrance of BR binding to the microspheres.

Effect of the pH. The adsorption percentage of BR (Figure 5) reached 92% at pH 7.4, 90% at pH 6.4, and 68% at pH 8.0. This showed that the best adsorption could be obtained near neutral conditions (pH 7), and a clear decrease in the adsorption was seen at alkalescent pH. This also showed the difference in the adsorption rate at different pHs: the fastest was at pH 7.4, it reached 79% at 0.5 h, and the rates were only 52 and 32% at pH 6.4 and 8.0, respectively.

The changes in the adsorption percentage with pH were mainly caused by electrostatic interaction between the adsorbents and BR. The main reason was that the degree of dissociation of the BR carboxylic acid groups (pK_a = 4.2–4.5) and the degree of protonation of the amino groups on the microspheres were strongly affected by the pH value. At the low pH of acidic conditions, BR carboxylic acid groups were nondissociated, so the BR molecule was uncharged. The electrostatic interaction between the microspheres and BR was very weak, although the amino groups on the microspheres were highly protonized, so the adsorption percentage was very low. The degree of dissociation of the BR carboxylic acid groups increased with increasing pH, whereas the degree of protonation of the amino groups on the microspheres decreased. These two cases resulted in an increase in electrostatic interaction when the pH was less than 7, so the adsorption rate increased. When the pH was about 7, the electrostatic interaction reached the maximum so that the adsorption rate reached the maximum. With increasing pH, the degree of protonization of amino groups on the microspheres further weakened until it disappeared. The electrostatic interaction obviously weakened. The adsorption rate was significantly reduced.

We concluded that the best pH for BR adsorption was 7.4. The normal pH value of blood is 7.35–7.45, with 7.4 being just in this range; this provides a favorable conditions for the clinical application of this sorbent in the future.

Effect of the Ionic Strength. It was found that the adsorption percentage decreased with increasing concentration of NaCl (Figure 6). The reason was that the carboxyl anions of the BR molecules at pH values of 7.2–7.4 were enriched around the positive ions to form an ion atmosphere in the solution. The concentration of the ion atmosphere increased with increasing ion strength. The presence of this ion atmosphere obstructed the contact between the carboxyl anions of BR and the amino cations on the microspheres, weakened the interaction between BR and the microspheres, and so decreased the effective concentration of BR in the solution. All of the previous results show that the increase of ion strength in the solution could inhibit the adsorption of BR on the adsorbents.

Effect of the Initial Concentration of BR. The equilibrium adsorption capacity increased and the equilibrium adsorption

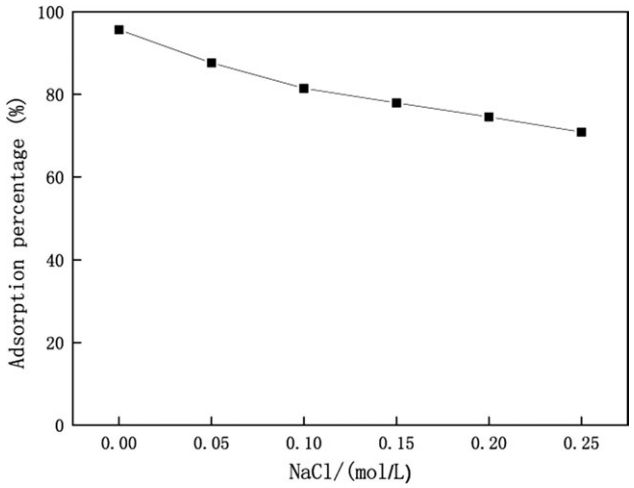

Figure 6. Effect of the ionic strength on the BR adsorption: BR initial concentration = 100 mg/L; BR solution volume = 10 mL; microsphere weight = 0.1 g; pH:7.2–7.4; phosphate buffer concentration = 0.05 mol/L; temperature = 37°C; time = 2 h; detected wavelength = 438 nm; microspheres = CS–G2.0, size of the microspheres = 80–100 mesh.

percentage decreased with increasing initial concentration of BR (Figure 7). The adsorption percentage was always over 90% when the initial concentration of BR increased from 50 to 350 mg/L. The adsorption percentage decreased to 85% when the initial concentration of BR increased further to 500 mg/L. The adsorption capacity increased from 5 to 43 mg/g and did not reach saturated adsorption when the initial concentration of BR was increased from 50 to 500 mg/L.

The equilibrium adsorption isotherm (Figure 8) showed that BR adsorption on the microspheres was a Langmuir monolayer adsorption and could be fitted and described with the following equation:

$$\log Q = n \log C + \log K, R^2 = 0.995$$

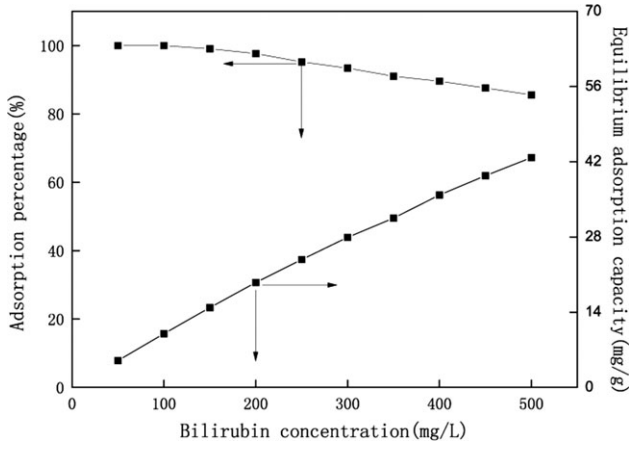

Figure 7. Effect of the initial concentration of BR on the adsorption: BR solution volume = 10 mL; microsphere weight = 0.1 g; pH 7.2–7.4; phosphate buffer concentration = 0.05 mol/L; temperature = 37°C; time = 4 h; detected wavelength = 438 nm; microspheres = CS–G2.0, size of the microspheres = 80–100 mesh.

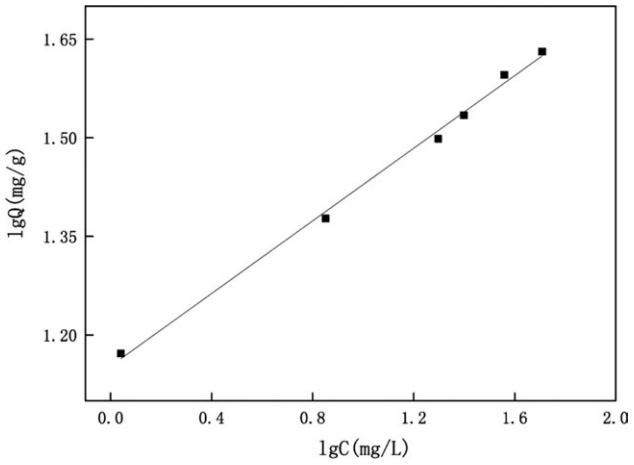

Figure 8. Adsorption Isotherm of CS–G2.0 Microspheres for BR. BR solution volume: 10 mL; microsphere weight: 0.1 g; pH: 7.2–7.4; phosphate buffer concentration: 0.05 mol/L; temperature: 37°C; detected wave length: 438 nm; microspheres = CS–G2.0, size of the microspheres = 80–100 mesh.

where Q is the equilibrium adsorption capacity (mg/g), C is the equilibrium concentration (mg/g), n and K are the physical constants of the Langmuir adsorption isotherm, and R is the correlation coefficient of the fitting.

Effect of BSA. Albumin is the natural carrier of BR in the blood. BR in the blood normally exists in the form of a combination with albumin. When the blood passes through the absorbent, both albumin and BR molecules can be adsorbed on the absorbent. If a large sum of protein in the blood is lost, a severe protein deficiency would appear; this is an important reason that most BR adsorbents cannot be applied in clinical treatment. In addition, the majority of BR in the blood is combined with albumin. There are 12 sites acting with BR in one albumin molecule, although only two of them are tightly integrated with the BR.[11] Therefore, adsorbents must possess a certain capacity of competition with albumin in the adsorption of BR in the blood. Therefore, in a study of adsorbents for BR in the blood, it is necessary to examine the efficiency of BR adsorption in the presence of albumin. In other words, we have to study whether this adsorbent can still absorb BR or how big its ability is to compete with albumin for BR adsorption to develop adsorbents that can be applied for clinical purposes.

One albumin molecule in the blood usually associates with one or two BR molecules, so in this study, the adsorption of BR on CS–G2.0 was investigated under three molar ratios of BSA to BR, that is, 1:1, 1:2, and 0:1 (Figure 9). Also, the adsorption for BSA on CS–G2.0 was studied under other three molar ratios of BSA to BR: 1:0, 1:1, and 1:2 (Figure 10). The aim was to further study the adsorption mechanism of BR on microspheres in the presence of BSA.

Figure 9 shows that the adsorption percentage in 5 h reached 52, 57, and 93% when the molar ratios of BSA to BR were 1:1, 1:2, and 0:1, respectively. The adsorption percentage and the adsorption rate for BR decreased with increasing concentration of BSA. The equilibrium time was delayed and exceeded 5 h in

Applied Polymer SCIENCE

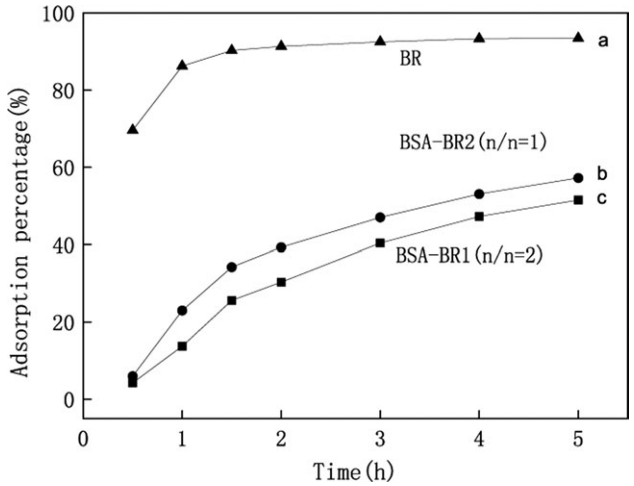

Figure 9. Effect of the BSA concentration on the BR adsorption: (a) in the absence of BSA, (b) n(BSA)/n(BR) = 0.5, (c) n(BSA)/n(BR) = 1. Initial concentrations: BR = 100 mg/L and (a–c) BSA, 5.814 g/L (b), 11.628 g/L (c). Solution volume = 10 mL, microsphere weight = 0.1 g, pH 7.2–7.4, phosphate buffer concentration = 0.05 mol/L, temperature = 37°C, detected wavelength: (a) 438 nm and (b,c) 460 nm, microspheres: CS–G2.0, size of the microspheres = 80–100 mesh.

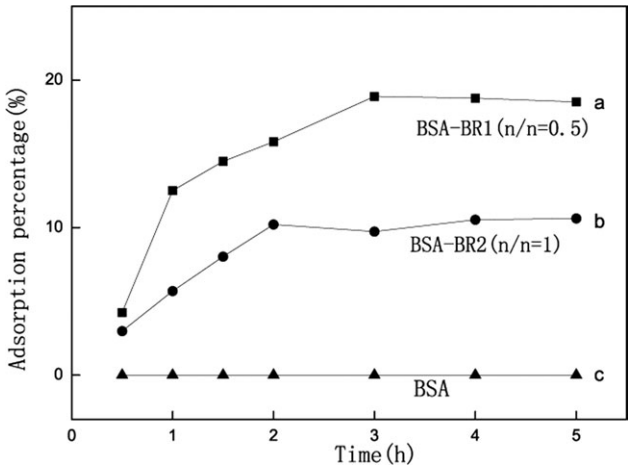

Figure 10. BSA adsorption dynamic curves on the CS–G3.0 microspheres: (a) n(BSA)/n(BR) = 0.5, (b) n(BSA)/n(BR) = 1, (c) in the absence of a BR initial concentration: (a,b) BR, 100 mg/L, (a) BSA, 5.814 g/L, and (b,c) 11.628 g/L. Solution volume = 10 mL, microsphere weight = 0.1 g, pH 7.2–7.4, phosphate buffer concentration = 0.05 mol/L, temperature = 37°C, detected wavelength = 292 nm, microspheres = CS–G2.0, size of the microspheres = 80–100 mesh.

the presence of BSA. There were three possible reasons. One was the much larger size of the complex of BR with BSA compared to that of BR; this reduced the diffusion speed of the complex to the microspheres. Another one was the massive volume of the complex, which decreased the opportunity for BR to contact the microspheres. In other words, it increased the steric hindrance of interactions between BR and the microspheres and blocked the diffusion of BR into the interior of microspheres. The last reason was the presence of the competitive adsorption of BR between BSA and the microspheres. With increasing BSA concentration, the adsorption of BR on BSA was enhanced, and thus, the adsorption of BR on the microspheres was weakened; this resulted in a decrease in the absorption percentage of BR.

Figure 10 shows that the adsorption percentages of BSA were 0, 11, and 19% when the molar ratios of BSA to BR were 1:0, 1:1, and 1:2, respectively. The adsorption of BSA onto the microspheres was very small under the previous three ratios, so this could not lead to the loss of a large sum of protein in the blood and severe protein deficiency. The adsorption percentage of BSA on the microspheres in the absence of BR was almost zero and was 11–19% in the presence of BR and increased with increasing molar ratio of BR to BSA. This was obviously because a small part of BSA combined with BR was indirectly absorbed onto the microspheres via the adsorption of BR. The adsorption of BSA onto the microspheres in the presence of BR reached equilibrium in 2–3 h, whereas the adsorption of BR in the presence of BSA did not reach equilibrium even after 5 h. This indicated that BR was still continuously dissociating from the combination with BSA and was absorbed onto the microspheres after 3 h, whereas no more BSA would be adsorbed along with the BR molecule to be adsorbed. This process continued until it reached equilibrium among the free BR, BR combined with BSA, and BR absorbed on microspheres. This showed that the microspheres had a good competitive ability for capturing the BR molecules even when they were combined with BSA.

The proposed materials in this study will be used for the adsorption of BR in blood in our future experiments. Their performance in blood purification, in issues such as safety and toxicity, mentioned in the Introduction, will be further evaluated.

CONCLUSIONS

A series of HDA-containing PAMAM dendrons supported on CS microspheres were synthesized by a divergent method in the preparation of PAMAM dendrimers. The amino content first increased then decreased with increasing generations. The adsorption behavior of BR on the microspheres was investigated in an aqueous solution. The adsorption percentages onto CS–G1.0 to CS–G4.0 were close to each other. The best adsorption conditions were pH 7.4, an ion strength of 0, and an equilibrium time of 2 h. The adsorption percentage increased with increasing temperature. Considering practical clinical application in the future, we fixed the adsorption temperature at 37°C. When the BR initial concentration was increased from 50 to 500 mg/L, the adsorption percentage decreased from 100 to 86%, with the adsorption capacity increasing from 5 to 43 mg/g and not yet reaching saturation. The adsorption percentage of BR decreased to a certain extent, and the equilibrium time was delayed with increasing BSA concentration. However, the adsorption percentage of BSA onto microspheres in the absence of BR was almost 0, and it was 11–19% in the presence of BR. The microspheres had a good competitive ability to capture and absorb BR combined with BSA.

ACKNOWLEDGMENTS

The authors thank Tianjin Scientific Grants (contract grant number 08JCYBJC11300) for financial support.

REFERENCES

1. Takahashi, K.; Umehara, Y.; Umehara, M.; Nishimura, A.; Narumi, S.; Toyoki, Y.; Hakamada, K.; Yoshihara, S.; Sasaki, M. *Ther. Apher. Dial.* **2008**, *12*, 264.
2. Naruse, K. *Artif. Organs* **2005**, *8*, 71.
3. Sauer, I. M.; Baurmeister, U. *Ther. Apher. Dial.* **2006**, *10*, 105.
4. Rozga, J. *Xenotransplantation* **2006**, *13*, 380.
5. Bachli, E. B.; Schuepbach, R. A.; Maggiorini, M.; Stocker, R.; Müllhaupt, B.; Renner, E. L. *Liver Int.* **2007**, *27*, 475.
6. Kurtovic, J.; Boyle, M.; Bihari, D.; Riordan, S. M. *Ther. Apher. Dial.* **2006**, *10*, 2.
7. Li, L. J.; Zhang, Y. M.; Liu, X. L.; Du, W. B.; Huang, J. R.; Yang, Q.; Xu, X. W.; Chen, Y. M. *Ther. Apher. Dial.* **2006**, *10*, 160.
8. Legallais, C.; Gautier, A.; Dufresne, M.; Carpentier, B.; Baudoin, R. J. Chromatogr. *B* **2008**, *861*, 171.
9. Onodera, K.; Sakata, H.; Yonekawa, M.; Kawamura, A. *Artif. Organs* **2006**, *9*, 17.
10. O'Grady, J. *Aliment Pharmacol. Ther.* **2006**, *23*, 1549.
11. Yu, Y. H.; He, B. L. *React. Funct. Polym.* **1996**, *31*, 195.
12. Shi, W.; Zhang, F. B.; Zhang, G. L. *J. Chromatogr. B* **2005**, *819*, 301.
13. Yi, Y.; Wang, Y. T.; Zhang, W. *J. Appl. Polym. Sci.* **2006**, *99*, 1264.
14. Zheng, C. J.; Huang, X. D.; Kong, L.; Li, X.; Zou, H. F. *Chin. J. Chromatogr.* **2004**, *22*, 128.
15. Lu, L.; Yuan, Z.; Shi, K. Y.; He, B. L. *Ion Exchange Adsorpt.* **2002**, *18*, 105.
16. Lu, L.; Yuan, Z.; Shi, K. Y.; He, B. L.; Liu, B.; Shen, B.; Wang, Q. S. *Chem. J. Chin. Univ.* **2003**, *24*, 454.
17. Zhang, K. S.; Sun, J. T.; He, B. L. *Chem. J. Chin. Univ.* **1999**, *20*, 965.
18. Denizli, A.; Kocakulak, M.; Piskin, E. *J. Chromatogr. B* **1998**, *707*, 25.
19. Xia, B. L.; Zhang, G. L.; Zhang, F. B. *J. Membr. Sci.* **2003**, *226*, 9.
20. Bayramoğlu, G.; Yalçın, E.; Arıca, M. Y. *Colloid Surf. A* **2005**, *264*, 195.
21. Yang, Y.; Long, Y. Y.; Cao, Q.; Li, K.; Liu, F. *Anal. Chim. Acta* **2008**, *606*, 92.
22. Syu, M. J.; Nian, Y. M. *Anal. Chim. Acta* **2005**, *539*, 97.
23. Syu, M. J.; Deng, J. H.; Nian, Y. M.; Chiu, T. C.; Wu, A. H. *Biomaterials* **2005**, *26*, 4684.
24. Baydemir, G.; Bereli, N.; Andaç, M.; Say, R.; Galaev, I. Y.; Denizli, A. *React. Funct. Polym.* **2009**, *69*, 36.
25. Baydemir, G.; Bereli, N.; Andaç, M.; Ridvan, S.; Galaev, I. Y.; Denizli, A. *Colloid Surf. B* **2009**, *68*, 33.
26. Zhang, L.; Jin, G. *React. Funct. Polym.* **2006**, *66*, 1106.
27. Jin, G.; Yao, Q. Z.; Zhang, S. Z.; Zhang, L. *Mater. Sci. Eng. C* **2008**, *28*, 1480.
28. Han, X. Y.; Zhang, Z. P. *Polym. Int.* **2009**, *58*, 1126.
29. Han, X. Y.; Zhang, Z. P. *Chem. J. Chin. Univ.* **2009**, *30*, 618.
30. Gao, B. J.; Lei, H. B.; Jiang, L. D.; Zhu, Y. *J. Chromatogr. B* **2007**, *853*, 62.
31. Ando, K.; Shinke, K.; Yamada, S.; Koyama, T.; Takai, T.; Nakaji, S.; Ogino, T. *Colloid Surf. B* **2009**, *71*, 255.
32. Yang, Z. P.; Si, S. H.; Fung, Y. S. *Thin Solid Films* **2007**, *515*, 3344.
33. Asano, T.; Tsuru, K.; Hayakawa, S.; Osaka, A. *Acta Biomater.* **2008**, *4*, 1067.
34. Wu, L. P.; Wu, W. H.; Li, Q.; Zhang, Q.; Wang, Y.; Lu, W.; Zhang, Z. P. *Macromol. Symp.* **2010**, *297*, 179.
35. Esfand, R.; Tomalia, D. A. In Dendrimers and Other Dendritic Polymers; Fréchet, J. M. J., Tomalia, D. A., Eds.; Wiley: New York, **2001**; p 587.
36. In Determination of Exchange Capacity of Anion Exchange Resin; National Bureau of Standards of the People's Republic of China; GB/T 5760–86; Standards Press of China: Beijing, **2000**.